ECS Transactions, 61 (15) 21-30 (2014)
10.1149/06115.0021ecst ©The Electrochemical Society

Breakthrough in Modeling of Electrodiffusion Processes; Continuation and Extensions of the Classical Work of Richard Buck

K. Szyszkiewicz[a], M. Danielewski[a], J. Fausek[a], J.J. Jasielec[b], W. Kucza[a], A. Lewenstam[a,b], T. Sokalski[b], and R. Filipek[a]
[a] Faculty of Materials Science and Ceramics, AGH University of Science and Technology, Kraków, Poland
[b] Abo Akademi University, Turku, Finland

In 1978 Brumleve and Buck published an important paper [1] pertaining to numerical modeling of electrodiffusion. At the time their approach was not immediately recognized and followed. However, it has changed since the beginning of 21st century.
The approach of Brumleve and Buck based on Nernst-Planck-Poisson (NPP) equations is utilized to model transient behavior of various electrochemical processes. Multi-layers and reactions allow extending applications to selectivity and low detection limit with time variability, influence of parameters (ion diffusivities, membrane thickness, permittivity, rate constants), and ion interference on ion-sensor responses. Solution of NPP inverse problem allows for optimizing sensor properties and measurement environment. Conditions under which experimentally measured selectivity coefficients are true (unbiased) and detection limit is optimized are demonstrated. Impedance spectra obtained directly from NPPs are presented. Modeling durability and diagnosis of reinforced concrete is presented. Chlorides transport in concrete is modeled using NPPs and compared to other solutions.

Introduction

The first really successful numerical modeling of electrodiffusion problems was presented in 1978 in the important paper by Timothy Brumleve and Richard Buck [1]. Novelty of their approach consisted of fully implicit method, non-uniform grids with two different types of finite differences (one for concentrations and second for fluxes) allowed to "*create an efficient computer algorithm which permits treatment of multi-ion systems, thick or thin cells (membranes), and interfacial kinetics*" [1].

In spite of the rapid increase of computational power at the time the paper was published their approach was not immediately recognized widely and followed by the electrochemical community. However, it has changed to some degree from the beginning of 21stcentury, e.g. [2, 3, 4, 5]. But still the majority of the present numerical modeling of electrodiffusion processes, for example, interpretations of ion-sensor response, determination of transient behavior of a system to electrical and chemical perturbations (electrochemical impedance spectra) focus on simplified models based on electroneutrality assumption, equivalent circuit models, equilibrium or steady-state, thus ignoring electrochemical migration and time-dependent effects, respectively. These theoretical approaches, due to their idealizations, make theorizing on ions distributions and electrical potential in space and time domains difficult or impossible.

For the above reasons, the approach of Brumleve and Buck based on Nernst-Planck and Poisson (NPP) equations is utilized here to model the transient behavior of various electrochemical processes. Additionally, including several layers and reaction terms in mass balance equation allows for extending the applications to such areas as: selectivity and the low detection limit with variability over time, influence of parameters, such as ion diffusivity, membrane thickness, permittivity, rate constants and primary to interfering ion concentration ratios on ion-sensor responses. Moreover solution of the NPP inverse problem allows searching for optimal sensor properties and measurement conditions. The conditions under which experimentally measured selectivity coefficients are true (unbiased) and detection limits are optimized are demonstrated, and practical conclusions relevant to clinical measurements and bioassays are derived [6].

Another important field of application includes modeling of durability and diagnosis of cement paste or reinforced concrete [7], [8]. Based on the extended NPP model electrochemical impedance spectra (EIS) can be generated and analyzed to predict steel and concrete corrosion and finally utilize to prevent material failure.

NPP model can be also a useful tool in the description of biological systems. The NPP model has the potential to reopen frontiers in the study of variety of the problems related to the electrochemistry of biological membranes [5], [9], [10].

The Nernst-Planck and Poisson model

Basically, two equations (mass balance and Poisson equation from electrostatics), flux constitutive expression, and boundary conditions constitute what is known as the Nernst-Planck-Poisson model. In 1D linear geometry with r species, the model is embodied in eqs. (1)-(5).

$$\frac{\partial c_i(x,t)}{\partial t} + \frac{\partial J_i(x,t)}{\partial x} = 0, \quad i = 1,\ldots,r;\ x \in [0,\mathrm{d}];\ \mathrm{t} \geq 0 \tag{1}$$

$$\frac{\partial E(x,t)}{\partial t} = \frac{1}{\varepsilon} I(t) - \frac{F}{\varepsilon} \sum_{i=1}^{r} z_i J_i(x,t) \tag{2}$$

$$J_i(x,t) = -B_i\, c_i(x,t) \left[\frac{\partial}{\partial x} (\mu_i(c_1,\ldots,c_r)) - z_i \cdot e \cdot E(x,t) \right] \tag{3}$$

where: E – the electric field, and J_i – the flux, c_i – the concentration, μ_i – the chemical potential, B_i – the mobility coefficient, z_i – the charge number of the *i-th* species. For thermodynamically ideal solutions ($\mu_i = \mu_i^{\circ} + RT \ln c_i$) and with Einstein–Smoluchowski relation ($D_i = kT B_i = \frac{RT}{N_A} B_i$) the flux (3) is reduced to the simpler form:

$$J_i(x,t) = -D_i \left(\frac{\partial c_i}{\partial x}(x,t) - \frac{F}{RT} z_i c_i(x,t) E(x,t) \right) \tag{4}$$

At each interface the boundary conditions must be specified. One possibility is the set of kinetic boundary conditions relating the fluxes to heterogeneous rate constants (k_i) and concentrations near interfaces:

$$\begin{aligned} J_i(d,t) &= -\vec{k}_{i,R} c_{i,R} + \overleftarrow{k}_{i,R} c_i(d,t), \\ J_i(0,t) &= \vec{k}_{i,L} c_{i,L} - \overleftarrow{k}_{i,L} c_i(0,t), \end{aligned} \tag{5}$$

where $\vec{k}_i$ are forward rate constants ("*to the membrane*"), $\overleftarrow{k}_i$ are backward rate constants ("*from the membrane*"), subscripts L and R indicate left ($x=0$) and right ($x=d$) boundary, respectively. Requirements (5) are usually referred to as *Chang-Jaffé boundary conditions [11]*.

Scaling and dimensionless variables

Introducing dimensionless variables, the number of the physico-chemical parameters can be reduced. Moreover, by finding the proper scaling factors it is possible to obtain better accuracy in numerical computations. Thus, the equations (1)-(5) are converted into a dimensionless form through the following transformations:

$$\bar{x} := x/x_s,\ \bar{t} := t/t_s,\ \bar{c}_i(\bar{x},\bar{t}) := c_i(x_s\bar{x}, t_s\bar{t})/c_s,\ \bar{E}(\bar{x},\bar{t}) := E(x_s\bar{x}, t_s\bar{t})/E_s, \qquad (6)$$

where x, t, c_i, E and $\bar{x}, \bar{t}, \bar{c}_i, \bar{E}$ are physical and dimensionless values of distance, time, concentration and electric field, respectively; x_s, t_s, c_s, E_s are their characteristic values (scaling factors). Dimensionless parameters take the form:

$$E_s = \frac{RT}{Fx_s},\quad k_s = \frac{x_s}{t_s}, \qquad (7)$$

After calculations we arrive at the following rescaled form of NPP system for $\bar{x} \in [0, \bar{d}]$

$$\frac{\partial \bar{c}_i}{\partial \bar{t}} = -\frac{\partial \bar{J}_i}{\partial \bar{x}}, \quad (i=1,\ldots,r); \quad \frac{\partial \bar{E}}{\partial \bar{t}} = \bar{I} - \lambda \sum_{i=1}^{r} z_i \bar{J}_i \qquad (8)$$

where: $\bar{I}(\bar{t}) = \frac{Ft_s x_s}{\varepsilon_0 \varepsilon_r RT} I(t_s\bar{t})$, $\bar{J}_i = -\bar{D}_i \frac{\partial \bar{c}_i}{\partial \bar{x}} + \bar{D}_i z_i \bar{c}_i \bar{E}$, $\lambda = \frac{c_s (F x_s)^2}{RT\varepsilon_r\varepsilon_0}$, $\bar{D}_i = D_i \cdot t_s / x_s^2$.

To ease the burden of notation we drop hereafter the over-bars in all quantities.

Numerical solution

Space discretization

The problem stated in above is straightforward to solve numerically using the method of lines. It consists of the space discretization using finite differences and solving the resulting system of ordinary differential equations (ODEs). To tackle the problem of large gradients a variable size grid is used, along with differences of second order accuracy which account for non-uniform grid. The numerical convergence is verified through multiple runs of different grid sizes.

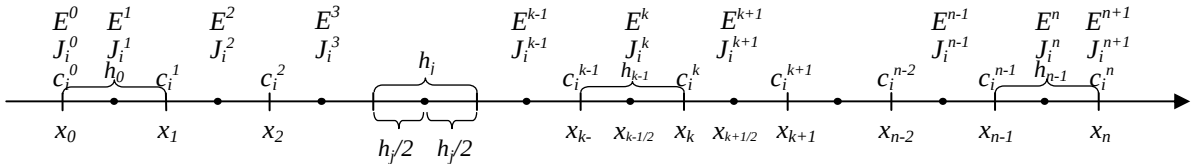

The schematic view of the space grid together with the location of concentrations, fluxes and electric field points are presented above. The general notation $c_i^k(t) := c_i(x_k, t)$, $E^k(t) := E(x_{k-1/2}, t)$, and $J_i^k(t) := J(x_{k-1/2}, t)$ is used in discretizations.

Convergence

One of the factors that have impact on the quality of numerical procedure is the order of local truncation error (LTE). It is reasonable to assume that the higher the order of LTE the better convergence is to be expected. The local truncation error LTE is a grid function defined as follows: if $(c_1,\ldots,c_r, E)(x,t)$ is the true solution of NPP problem, then we can calculate the value of the finite difference expression after substituting into it this true solution. Now the LTE measures how well the true solution satisfies the difference scheme. In other words the LTE measures the error introduced by the evaluating the finite difference expression instead of evaluating the right-hand side of the equations. Derivation of the LTE both for Brumleve-Buck [1] and our approach was carried out revealing the following estimates [12].

$$\begin{aligned} &\textit{Brumleve Buck}: && LTE = O\left(\frac{2(h_{k-1}+h_k)}{h_{k-2}+2h_{k-1}+h_k}-1\right)+O(\delta), \\ &\textit{Our method}: && LTE = O(h_k - h_{k-1})+O(\delta^2), \end{aligned} \tag{9}$$

where $\delta = \max\{h_k\}$. Thus, for our method $\lim_{\delta\to 0} LTE = 0$ which means consistency. In the case of Brumleve-Buck $\lim_{\delta\to 0} LTE = 0$ but only if additional conditions are imposed (for instance, $h_k / h_{k-1} \to 1$). Moreover the LTE approximation is one order higher for our method.

Extensions

In comparison to original paper of Brumleve & Buck [1] the following extensions substantially enlarge NPP model towards practical applications:

1) Introduction the reactive terms (source/sink) to the NPP problem in continuity equation:

$$\frac{\partial c_i}{\partial t} = -\frac{\partial J_i}{\partial x} + R_i(c_1,\ldots,c_1,E) \tag{10}$$

2) Introduction multi-layers to NPP problem:

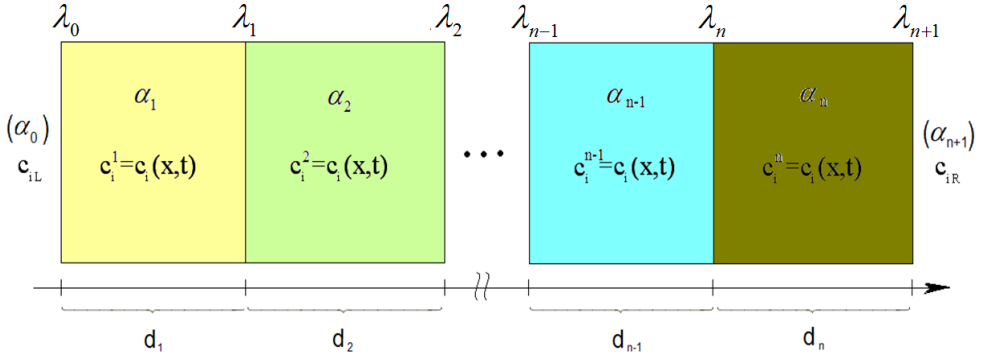

$$\begin{cases} \dfrac{\partial c_i^j}{\partial t}(x,t) = -\dfrac{\partial J_i^j}{\partial x}(x,t) \ \ (i=1,\ldots,r), \ \ \dfrac{\partial E^j}{\partial t}(x,t) = \dfrac{1}{\varepsilon_j} I(t) - \dfrac{F}{\varepsilon_j}\sum_{i=1}^{r} z_i J_i^j(x,t), \\ x \in [\lambda_{j-1},\lambda_j] \ \ \text{for each layer} \ \ j=\alpha_1,\ldots,\alpha_n, \ \ t \in [0,t_{END}], \end{cases} \tag{11}$$

with $J_i^j(x,t) = -D_i^j \dfrac{\partial c_i^j}{\partial x}(x,t) - \dfrac{F}{RT} D_i^j z_i (c_i^j E^j)(x,t)$ in each layer.

Detection limit of ISE

As the NPP model is a general method to describe electrodiffusion processes, which lead to the formation of the membrane potential, thus it is able to take into account several parameters of ion-selective electrodes (ISEs) which are not addressed in simpler models. This section presents NPP modeling of detection limit of ISE (a comparison between the NPP model and simpler models and influence of various parameters on the detection limit of ISEs are discussed extensively elsewhere, [13]) by showing direct predictions of the models (Fig. 1) and also by inverse modeling (Fig. 2). Consequently it allows finding out the values of physical parameters which produce the desired detection limit.

Selectivity (K_{IJ}) and detection limit (DL) are basic parameters of all ion-selective electrodes. Models describing ISE behavior – and in consequence K_{IJ} and DL – are still subject of a current debate. There are two main positions: the first one opts for simplicity while the other one stresses generality [6].

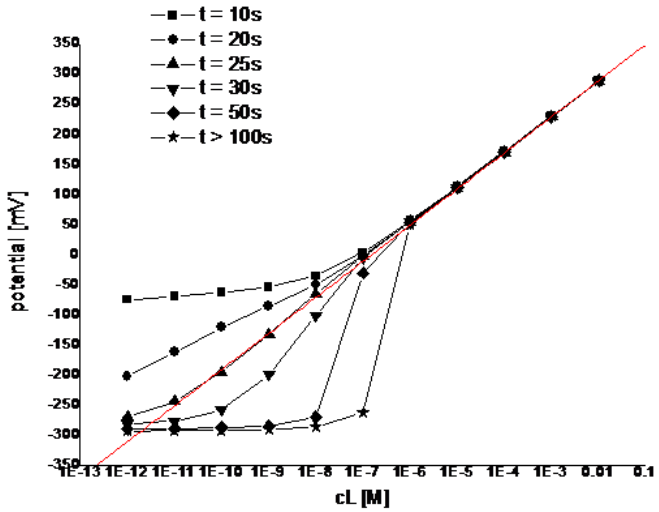

Fig. 1. Influence of measuring time for the ISE with preferred ion inner solution concentration 10^{-10} obtain using the NPP model.

The cases described so far are of the direct type: compute the value of the detection limit for given parameters. But we can also pose an *inverse problem* namely: identify a set of parameters which give the best detection limit. A definition of the target function *Err* to be optimized was based on the calibration curves, eq. (12). These curves show dependence of the steady state potential $(\varphi_{ss} = \lim_{t\to\infty} \varphi(t))$ of ISE against logarithm of the primary ion concentration (for instance see Fig. 1). To obtain steady state value φ_{ss} one can solve the NPP system for times long enough to have solution not changing in time and use formula $\varphi(t) = -\int_0^d E(x,t)dx$ relating the electric field and potential.

$$Err(\{D_i\},\{k_i\},d) = \int_{c_{\min}}^{c_{\max}} |\varphi_{ss}(\log c;\{D_i\},\{k_i\},d)) - \varphi_{\mathrm{ss,experiment}}(\log c)|^2 \, dc \qquad (12)$$

However, in the case of detection limit one can perform the optimization procedure entirely within the model (not resorting to experiments) by defining the target function as the length of the linear part on the calibration curve (Fig. 1). The answer to

this problem is illustrated in Fig. 2 which shows contour plot of the detection limit vs. the measurement time and the concentration of the primary ion in the inner solution.

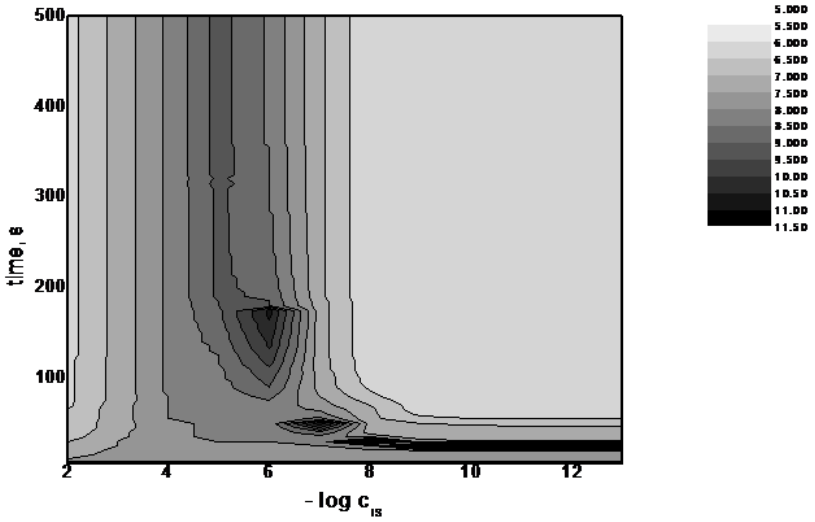

Fig. 2. The time–concentration-detection limit maps obtained using the NPP model.

Electrochemical Impedance Spectroscopy (EIS)

Electrochemical impedance spectroscopy (EIS) is a useful tool for analyzing electrochemical systems mainly because it allows the separation and characterization of individual kinetic processes. Calculating for the first time the impedance spectra for any number of species without electroneutrality assumption was another important contribution of Buck and Brumleve.

In general the impedance may be obtained from the linear response to a small perturbation, Fig 3. NPP model can also be used for the interpretation of electrochemical impedance spectra of ion-sensors using the analogy-type concept of the *"equivalent" electric circuit* but directly addressing the physicochemical properties of the sensors modeled and relating the transport properties of the bulk and interfaces (diffusivities, heterogeneous rate constants of transport across interfaces) to the characteristic features of complex impedances.

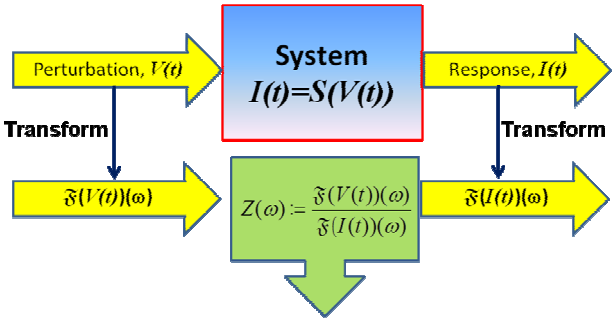

Fig 3. The EIS schema – in a regime of *linearity* and time-invariance the function $Z(\omega)$ does not depend on $V(t)$ and characterizes the system, [14] pp. 450–457.

The standard method for obtaining impedance spectrum $\{Z(\omega) = (Z'(\omega), Z''(\omega))\}_{\omega>0} \subset \square$, both in numerical simulations and real-world experiments, is to subject a system to the sinusoidal perturbation $I(t) = I_0 \sin \omega t$ with

frequency ω and next to record (after some relaxation period) the sinusoidal response $V(t) = V_0 \sin(\omega t - \phi)$. This will produce one point (for a given ω) of the spectrum: $Z(\omega) = (\frac{V_0}{I_0}\cos\phi, \frac{V_0}{I_0}\sin\phi) \in \square$. Usually about 60–120 points are enough to get a desired spectrum. In numerical simulations it means that one must run the program repeatedly 60–120 times. Here, again Brumleve and Buck provided interesting improvement allowing for one-run method to obtain full spectrum. In the paper this approach for EIS simulations is adopted. At first, under zero total current density (open-circuit) simulations are carried out until the steady state is obtained. Then the system is perturbed by a step current:

$$I(t) = \begin{cases} I_0 & \text{for } t \geq 0, \\ 0 & \text{for } t < 0. \end{cases} \tag{13}$$

where I_0 is the amplitude of the current small enough ($\sim 10^{-4} A$) to retain the linearity regime. Computations are carried out until the new steady state is reached ($t \sim 10^4 s$). The Fourier transform of the potential-time function, $(0,\infty) \ni t \mapsto V(t)$ allows the complex impedances to be determined:

$$V'(\omega) = \int_0^\infty (V(t) - V_\infty)\cos(\omega t)dt, \quad V''(\omega) = \int_0^\infty (V(t) - V_\infty)\sin(\omega t)dt + V_\infty / \omega, \tag{14}$$

where $V_\infty = \lim_{t\to\infty} V(t)$. Using the analytical form of the Fourier transform of the step function perturbation, (13), one has the impedance components: $Z'(\omega) = -V''(\omega)\cdot\omega / I_0$, $Z''(\omega) = V'(\omega)\cdot\omega / I_0$.

Fig. 4 shows EIS simulations with $r = 3$ ionic species for ion-selective membrane in contact with a bathing solution containing a primary ion for different cationic transfer rates at the membrane interfaces. The case presented assumes full dissociation in the homogenous membrane (no reaction terms were used). Both interfaces block the third ion: $\vec{k}_{3,L} = \overleftarrow{k}_{3,L} = \vec{k}_{3,R} = \overleftarrow{k}_{3,R} = 0$.

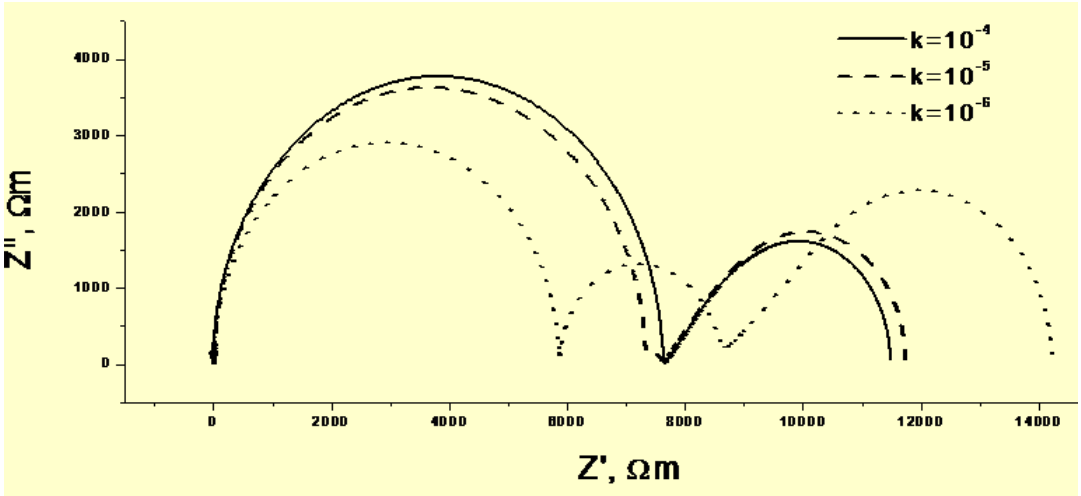

Fig. 4. Typical examples of simulated complex impedances for heterogeneous rate constants k = 10^{-4}, 10^{-5}, 10^{-6} ms^{-1}. The membrane width d = 200 μm, diffusion coefficients: D_1=10^{-10}, D_2=D_3=10^{-11} m^{2}s^{-1}. The relative permittivity $\varepsilon_r = 80$ (as for pure water) and charge numbers $z_1 = +2$, $z_2 = +1$, $z_3 = -1$.

Transport processes in concrete; a certain method of determination of diffusion coefficients

The process of ionic electrodiffusion remains also important in some civil engineering problems. For instance, the long-term durability of many construction materials, such as reinforced concrete, is directly affected by the transport of chemical species. Corrosion of reinforcing steel due to exposure to chloride leads to degradation of steel reinforced concrete structures.

Transport of ions inside a concrete is commonly assumed to be governed by Fick's law of diffusion. However, during testing of chloride diffusivity what is often observed cannot be satisfactorily elucidated by Fick's law. Long term testing – see schematic view in Fig. 5 – are often explained by assuming that the apparent diffusivity is not constant [15]. But what is almost universally ignored in this field is the fact that most species contained in cement paste or concrete are ionic, [16], (for example Cl^-, OH^-, Na^+, K^+, Ca^{2+}), and electric field cannot be neglected – hence the NPP equations form more accurate description.

Steel rebars in reinforced concrete are protected against corrosion due to alkaline reaction of concrete layer. Transport of aggressive ions, e.g., Cl^- results in corrosion of steel in concrete and shortens the life time of a construction. To assess the chloride diffusivity a two chamber device is used, Fig. 5. Very simple model (steady state, space constant flux, electroneutrality) leads to the following solution

$$c_2(t) = c_2(0)\exp(-\frac{DA}{V_2\ell}t) + \frac{DA}{V_2\ell}\int_0^t c_1(s)\exp(\frac{DA}{V_2\ell}(s-t))ds, \qquad (15)$$

which upon knowing $c_1(t)$ and $c_2(t)$ can be easily used for retrieving D. This may even be more simplified as usually one chamber "1" contains highly concentrated solution of Cl^- so $c_1(t) = c_1 = const$, and then (15) is converted to $\ln(1-c_2(t)/c_1) = -\frac{DA}{V_2 l}t$.

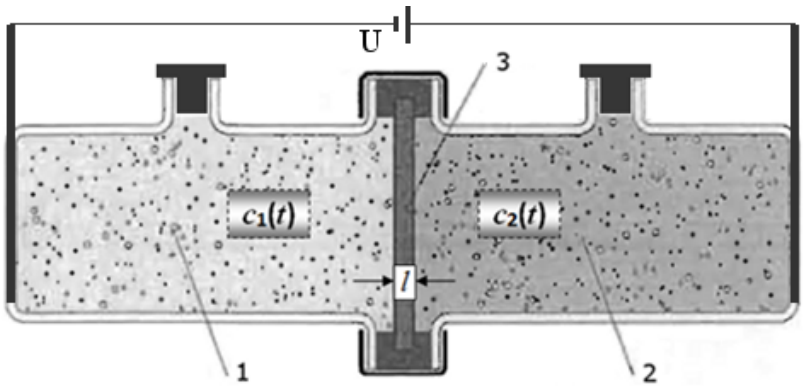

Fig. 5. Scheme of equipment used for chloride diffusion measurement: 1, 2 – two chambers where the concentration of chloride ions are controlled (V_2 – the volume of chamber 2); 3 – the concrete sample of width l and area A. U – applied voltage (in the case of rapid diffusion measurement).

Here again the NPP model provides better understanding and more accurate results especially in rapid chloride diffusion measurement by applying external field to speed up the process, see Fig. 5 where U is the applied voltage. While in this case the electric field in the sample cannot be ignored hence authors neglect the diffusion term and postulate the linear electric potential in the sample [17]:

$$\frac{\partial c^{Cl^-}}{\partial t} = -\frac{\partial j^{Cl^-}}{\partial x}, \quad j^{Cl^-} = \frac{z^{Cl^-} F}{RT} D^{Cl^-} c^{Cl^-} \frac{\partial \varphi}{\partial x}, \; \varphi(x) = U \cdot \left(1 - \frac{x}{\ell}\right) \tag{16}$$

The inverse method based on the error function

$$Err(\{D_j\}) = \sum_{i=1}^{r} \int_0^{\ell} | c_i(x, t^*, \{D_j\}) - c_{i,\exp.}(x, t^*) |^2 \; dx. \tag{17}$$

for the case $i \in \{Cl^-, OH^-, Ca^{2+}\}$ gave the results:

Time, t*, [h]	$D_{Cl^-} \cdot 10^{12}$ [$m^2 s^{-1}$] Simplified model [**Error! Bookmark not defined.**]	$D_{Cl^-} \cdot 10^{12}$ [$m^2 s^{-1}$] NPP model
24	0.69	0.76
48	0.63	0.70
72	0.41	0.54

Conclusions

- The Nernst-Planck-Poisson (NPP) model is physically relevant and effective method of electrodiffusion processes description.
- The NPP model can be used to predict time dependent and steady-state solutions: e.g., the variability of selectivity, low detection limit and other parameters [13], [18], [19].
- All-solid-state ISEs with conducting polymer can be theoretically described using a multilayer NPP model [18].
- The NPP model opens new possibilities in the modeling and understanding of electrodiffusion processes in various applications, e.g.: membrane potential formation, transport processes in concrete, biological membranes, in routine clinical analysis [19] etc.

Acknowledgments

This work was supported by the Polish National Centre for Research and Development Grant No. K1/IN1/25/153217/NCBiR/12.

References

[1] T. Brumleve, R. Buck, *J. Electroanal. Chem.* **90** (1078) 1-31.
[2] T. Sokalski, A. Lewenstam, *Electrochem. Commun.* **3** (2001) 107.
[3] T. Sokalski, P. Lingenfelter, A. Lewenstam, *J. Phys. Chem. B* **107** (2003) 2443.
[4] E. J. F. Dickinson, L. Freitag and R. G. Compton, *J. Phys. Chem. B* **114** (2010) 187.
[5] C.L. Gardner, W. Nonner, R.S. Eisenberg, *J. Comp. Electron.* **3** (1), (2004) 25-31.
[6] J. Bobacka, A. Ivaska, A. Lewenstam, *Chem. Rev.* **108** (2008) 329.
[7] E. Samson; J. Marchand, *Int. J. Numer. Meth. Engin.*, **1999**, 46, 2043–2060.
[8] J. Xia, Long-yuan Li, *Constr. and Building Mat.* 39 (2013) 51–59.
[9] S. Furini, F. Zerbetto, S. Cavalcanti, *Biophy. J.* **91** Nov. 2006, 3162–3169.
[10] R.D. Coalson, M.G. Kurnikova, *IEEE Trans. NanoBioSci*, vol. **4**, no. 1, (2005).

[11] H. Chang, E. Jaffé, *J. Chem. Phys.* **20** (1952) 1071–1077.
[12] J.J. Jasielec, K.Szyszkiewicz, R. Filipek, J. Fausek, M. Danielewski, A. Lewenstam, *Comp. Mat. Sci.* **63** (2012), 75–90.
[13] J.J. Jasielec, T. Sokalski, R. Filipek, A. Lewenstam, *Electrochim. Acta* **55** (2010) 6836–6848.
[14] A. Quarteroni, R. Sacco, F. Saleri, *Numerical Mathematics*, Springer, Texted in Applied Mathematics (2000).
[15] T. Zhang, O.E. Gjørv, *Cem. and Conc. Res.*, vol. **26**, no. 6, (1996) 907–917.
[16] S. Chatterji, *Cem. and Conc. Res.*, vol. **25**, (2), February 1995, 299–303.
[17] A. Zybura *at. al*, *Arch. Civ. Eng. Envir. (ACEE)*, no. **1** (2012), 55–62.
[18] J.J. Jasielec, G. Lisak, M. Wagner, T. Sokalski, A. Lewenstam, *Electroanalysis*, no. **1**, 25, (2013) 133–140.
[19] A. Lewenstam, *Electroanalysis*, **26** (6), (2014), 1171–1181, [doi: 10.1002/elan.201400061].